Seventh International Symp. on Magnetic Bearings, August 23-25 , 2000, ETH Zurich

GAIN SCHEDULED ADAPTIVE VIBRATION CONTROL

Felix Betschon
Swiss Federal Institute of Technology, Technoparkstr Zurich, betschon@eek.ee.ethz.ch

Carl Knospe
University of Virginia, Charlottesville, VA, USA, crk4y@virginia.edu

ABSTRACT

A new method for the reduction of either the vibration or AMB current induced by rotor imbalance is presented. The approach is based on previous research on Adaptive Vibration Control for active magnetic bearing systems. To minimize the memory and computational requirements imposed on the hardware, the gain matrix used is synthesized as functionally dependent upon the operating speed with only the diagonal elements varying linearly with speed. The resulting algorithm was experimentally tested on a high-speed spindle. Significant reductions in bearing currents were achieved over a wide range of operating speeds.

INTRODUCTION

For many proposed applications of magnetic bearings (AMB), system costs are critical to marketability. Of the system components, the power electronics' costs are becoming increasingly dominant since progress has been slower in the integration of power electronics than in the signal electronics. One effective mean to reduce the costs of the power electronics is to minimize the AMB's power consumption and the reactive power required. If a rotor is perfectly symmetrical, the axis of inertia and the geometric axis are identical. In this case, the rotor turns around its geometric axis and the measured vibration is zero (the shaft orbit is a single point). Of course, actual rotors are never perfectly symmetrical and this results in the geometric and inertial axes being not coincident. In this case, the shaft will orbit when rotating. The feedback controller acts to oppose this vibration, resulting in a significant synchronous component to the control current. Typically, this imbalance-induced synchronous component is the dominant part of the AMB control current. To minimize the AMB power consumption and reactive power required, this synchronous component needs to be greatly reduced.

Two different but related methods may be used to accomplish this:

1) a synchronous notch filter in the feedback controller
2) feedforward cancellation

Tracking notch filters [2] may be inserted directly into the closed loop. However they have the disadvantage that it is difficult to design them to operate over a wide range or near bending criticals. The idea of feedforward control is to add compensation signals to the closed loop system. The feedback controller can be developed without considering this feedforward algorithm. It should be pointed out that adaptive feedforward strategies are closely related to generalized notchfilters [2]. However the synthesis techniques for adaptive feedforward control are significantly more straightforward.

THEORY OF GAIN-SCHEDULED ADAPTIVE VIBRATION CONTROL

The feedforward technique used herein, known as *Adaptive Vibration Control (AVC)*, was developed by the second author and has been extensively studied ([3]-[7] and references therein). The basic principle is illustrated in Figure 1.

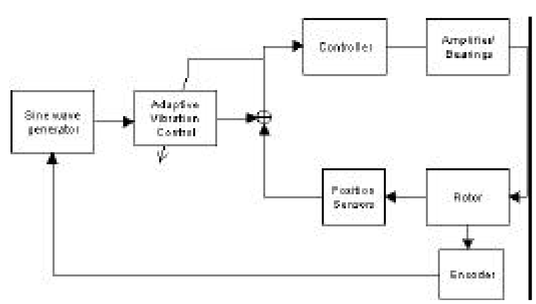

Figure 1. Structure of the control loop

The following quasi-static model of the rotor's synchronous response is the basis for adapting the feedforward signals,

$$\boldsymbol{x} = \boldsymbol{T}\boldsymbol{u} + \boldsymbol{x}_0 \qquad (1)$$

where $\boldsymbol{x}$ represents the $2n \times 1$ real vector of synchronous Fourier coefficients of the n performance signals, $\boldsymbol{u}$ the $2m \times 1$ vector of synchronous Fourier coefficients of m feedforward signals applied to the magnetic bearing, $\boldsymbol{T}$ is the $2n \times 2m$ real-valued transfer matrix of the feedforward signals to the performance signals and $\boldsymbol{x}_0$ is the $2n \times 1$ real vector of synchronous Fourier coefficients of the performance signals, when no feedforward signals are applied. The factor 2 in the vector size arises from the conversion of each complex Fourier coefficients to two real numbers. In the above discussion, a performance signal is a signal of which we wish to reduce the synchronous component. The feedforward signal may be added to either the feedback controller's output or the rotor's position measurement signals. In the case presented here, the AVC input is inserted before the position controller and seeks to minimize the synchronous component of the input signals delivered to the feedback controller. Because the timebase for calculating the schedule for future compensation signals is much longer than a feedback controller cycle, this method can be considered as an open loop control. Thus the AVC does not affect the system stability and the position controller can be designed with the AVC neglected.

$$J = \boldsymbol{x}^* \boldsymbol{x} \qquad (2)$$

The AVC seeks to minimize the quadratic performance function (2). Substitution of (1) into (2) and taking the first derivative with respect to the control vector $\boldsymbol{u}$ yields:

$$\frac{dJ}{d\boldsymbol{u}} = \boldsymbol{u}^* \boldsymbol{T}^* \boldsymbol{T} + \boldsymbol{x}_0 \boldsymbol{T} \qquad (3)$$

The optimal control vector can be determined by setting (3) equal to zero and solving it for $\boldsymbol{u}$. This results in the global control law:

$$\boldsymbol{u} = -(\boldsymbol{T}^* \boldsymbol{T})^{-1} \boldsymbol{T}^* \boldsymbol{x}_0 \qquad (4)$$

Note that this depends on the uncontrolled performance signal being set to zero, which is undesirable. An alternative to this control law is to use a recursive formulation. For this we introduce the subscript i for the Fourier coefficients determined from several (10 to 20) recent rotor revolutions. By taking the difference between $\boldsymbol{x}_i$ and $\boldsymbol{x}_{i+1}$ the uncontrolled vibration $\boldsymbol{x}_0$ can be eliminated from the quasi-static model:

$$\boldsymbol{x}_{i+1} - \boldsymbol{x}_i = \boldsymbol{T}(\boldsymbol{u}_{i+1} - \boldsymbol{u}_i) \qquad (5)$$

Now once again the optimal control vector can be eliminated by minimizing the performance signal yielding the *local control law*:

$$\boldsymbol{u}_{i+1} = \boldsymbol{u}_i + \boldsymbol{A}\boldsymbol{x}_i \qquad (6)$$

with the *optimal adaptation gain matrix*:

$$\boldsymbol{A} = -(\boldsymbol{T}^* \boldsymbol{T})^{-1} \boldsymbol{T}^* \qquad (7)$$

Note that the matrix $\boldsymbol{T}$ is a function of operating speed and hence the gain matrix $\boldsymbol{A}$ will also be so. We shall denote the matrix $\boldsymbol{T}$ for operating speed ω_k by $\boldsymbol{T}_k$. Furthermore, $\boldsymbol{A}_k$ will indicate the gain matrix used at speed ω_k. The matrix $\boldsymbol{A}_k$ need not be chosen to be $-(\boldsymbol{T}_k^* \boldsymbol{T}_k)^{-1} \boldsymbol{T}_k^*$ for the algorithm to be effective. For example, in the typical case where $m = n$ (number of performance signals equal to the number of feedforward control signals) the local control law will completely eliminate the synchronous component with any gain matrix $\boldsymbol{A}$ as long as the adaptation is stable (see below). In this case, the optimal matrix is given by

$$\boldsymbol{A}_{opt} = -\boldsymbol{T}^{-1} \qquad (8)$$

For the remainder of this paper, we will restrict our development to the case where $m = n$ as it is in our application. The transfer matrices $\boldsymbol{T}_k$ may be determined either through a system model or through experimental identification. The result of both methods is a set of transfer matrices. We will assume throughout this paper that this set of matrices is a representative of all the matrices for a speed range. It is relatively easy to collect enough transfer matrices with suitably spaced frequencies such that the set satisfies this assumption.

Reducing the number of adaptation gain matrices

Using equations (5) and (6), it is easy to derive the following simple sufficient condition for adaptation stability [6]:

$$\bar{\sigma}(\boldsymbol{I} + \boldsymbol{A}_k \boldsymbol{T}_k) < 1 \qquad (9)$$

where $\bar{\sigma}(\ldots)$ denotes the maximum singular value.

An obvious method for implementing the AVC control is to calculate $\boldsymbol{A}_k = -\boldsymbol{T}_k^{-1}$ and store these values in a look-up table with some interpolation of these gain matrices for speeds between the ω_k's. This method has been widely implemented and yields quick elimination of the synchronous components, as the optimal gain matrix for each speed is used. A disadvantage of this approach is the large memory space which is necessary for storing the $\boldsymbol{A}_k$'s, especially for rotors operating over a wide speed range. This increases the cost of the signal electronics.

A number of strategies have been advocated for reducing the number of matrices required [7] including:

1) synthesizing a single gain matrix **A** which satisfies (9) for all frequencies in the speed range
2) synthesizing a gain matrix which is functionally dependent on operating speed (implicit gain scheduling)

A single matrix has the advantage that minimal memory is necessary and no additional computation associated with speed dependence is needed. In this case the matrix $\boldsymbol{A}$ has to satisfy the following inequality:

$$\bar{\sigma}(\boldsymbol{I} + \boldsymbol{A}\boldsymbol{T}_k) < \gamma < 1 \qquad (10)$$

for each speed ω_k. Here, γ is the inverse of the adaptation convergence rate. Using Schur complement, each of these conditions can be transformed to a linear matrix inequality (LMI). This is a convex feasability problem and may be easily solved using available software.

$$\begin{bmatrix} \gamma\boldsymbol{I} & \boldsymbol{I} + \boldsymbol{A}\boldsymbol{T}_k \\ (\boldsymbol{I} + \boldsymbol{A}\boldsymbol{T}_k)^* & \gamma\boldsymbol{I} \end{bmatrix} > 0 \qquad (11)$$

If the $\boldsymbol{T}_k$'s vary strongly from each other a single gain matrix $\boldsymbol{A}$ that satisfies (11) for all $k = 1, \ldots, N$ covering the operating speed range may not exist. Indeed, this is the case for the experimental rotor discussed in the next section.

To synthesize a gain matrix that is functionally dependent on operating speed, a finite basis must be chosen for the function. For on-line computational simplicity, the affine matrix function

$$\boldsymbol{A}_k = \boldsymbol{A}_0 + \omega_k \boldsymbol{A}_1 \qquad (12)$$

is chosen here. The task of gain matrix function synthesis then is to determine $\boldsymbol{A}_0$ and $\boldsymbol{A}_1$ so that (9) holds for all ω_k. To further simplify the real computation for the adaptation presented here, the matrix $\boldsymbol{A}_1$ was chosen to have the form

$$\boldsymbol{A}_1 = a_1 \boldsymbol{I} \qquad (13)$$

after it was noted from experimental data that the diagonal elements of $\boldsymbol{T}_k$ were undergoing the greatest variation with speed for the test rig considered. This reduces the number of operations to calculate $\boldsymbol{u}_{i+1}$ as Table 1and Table 2 show:

Table 1: Number of operations to calculate $\boldsymbol{u}_{k+1}$ with any $\boldsymbol{A}_1$

$\boldsymbol{u}_{k+1}=$	$(\boldsymbol{A}_0 +$	$\omega_k \cdot \boldsymbol{A}_k$	$\cdot\, \boldsymbol{x}_k$	$+\boldsymbol{u}_k$	Total
Additions:	$4n^2$		$4n^2$-$2n$	$2n$	$8n^2$
Multiplications:		$4n^2$	$4n^2$		$8n^2$

Table 2:. Number of operations to calculate u_{k+1} with $A_1=a_1 I$

$\boldsymbol{u}_{k+1}=$	$\boldsymbol{A}_0 \cdot \boldsymbol{x}_k$	$+$	$\omega_k \cdot a_1 \boldsymbol{I}$	$\cdot\, \boldsymbol{x}_k$	$+\boldsymbol{u}_k$
Additions:	$4n^2$-$2n$	$2n$			$2n$
Multiplications	$4n^2$		1	$2n$	

This choice also reduces the memory required by almost 50%. In this case, the condition (9) can be stated as:

$$\begin{bmatrix} \gamma\boldsymbol{I} & \boldsymbol{I} + (\boldsymbol{A}_0 + \omega_k a_1 \boldsymbol{I})\boldsymbol{T}_k \\ (\boldsymbol{I} + (\boldsymbol{A}_0 + \omega_k a_1 \boldsymbol{I})\boldsymbol{T}_k)^* & \gamma\boldsymbol{I} \end{bmatrix} > 0 \qquad (14)$$

The synthesis task is then to determine $\boldsymbol{A}_0$ and a_1 such that condition (14) is satisfied for all ω_k. Since the constraint for each ω_k is convex, the synthesis problem is a convex feasibility problem. Furthermore, if we chose to minimize γ (i.e. maximize convergence rate) this synthesis is a generalized eigenvalue problem (GEVP) [1] and is a convex optimization problem. This can be solved using the LMI toolbox of MATLAB.

Test Rig and Electronics used

To examine these current minimizing strategies, they were tested on a high-speed AMB spindle (Fig. 2) designed for a maximum speed of 120'000rpm (2kHz). Because the motor control is still under development, operation above 90'000rpm (1.5kHz) is not possible at this time.

The rotor has a length of 180mm and an average diameter of approximately 30mm. It has its first free-free bending mode at 1650Hz and is not very gyroscopic. The rotor consists of two radial bearing journals, an axial bearing disk and a permanent magnet motor rotor that is held in place with carbon fibres. The total weight of the rotor is 680g.

The position of the rotor is measured in each of the five bearing axes by eddy-current sensors. At one end of the rotor a diametrically magnetized permanent magnet is mounted. Hall sensors measure its field in x- and y-axes, which gives a speed-synchronous sine and a cosine signal locked to the shaft rotation. These signals are directly used by the AVC algorithm for convolution. This hardware solution relieves the signal processor from having to generate these signals.

This digital signal processor, a TMS320C50 of Texas Instruments, constitutes the heart of the signal electronics. It is a 16-bit fixed point processor with a clock rate of 80MHz. The signal electronics has 7

Figure 2. High-speed spindle

analog inputs: 5 for the eddy current sensor signals and 2 for the Hall sensor signals.

The power electronics consists of 5 H-bridges. Each of them delivers a maximum output current of 2.5A at 48V with a PWM-frequency of 62.5kHz.

The feedback control algorithm used is of conventional PID type with the D-term produced by lead-lag elements.

Implementation

The control algorithms (feedback and AVC) are implemented on the TMS320C50 a 16-bit fixed point processor. The programming was done in Assembler to eliminate the unnecessary overhead often produced by compilers so as to achieve fast execution. Unfortunately, using a fixed point processor means scaling internal variables, and a great deal more programming effort is required, for example for a division operation.

Adaptive Vibration Control

The entire adaptation process is transacted in the Fourier domain. Therefore, the first element of AVC (see 4) is a convolution of the four performance signals with a sine and a cosine of the same frequency as the rotating speed, here produced by the hall sensor. This convolution results in an 8×1 vector of Fourier coefficients of the sensor signals (since there are four radial vibration measurements). This vector is sampled with a much lower frequency than that used for the discrete time convolution.

The actual adaptation process consists of a matrix multiplication and a discrete-time integration (see equation (6) and Fig. 3). First $\boldsymbol{A}(\omega)$ must be calculated from (12). This consists of 1 multiplication and 8 additions. The Fourier vector of the sensor signals is then multiplied by this 8×8 matrix. This step consists of 64 additions and 64 multiplications. Although the DSP executes one addition and one multiplication in a single clock cycle, this step is still quite time-consuming. The vector after the discrete-time integration then are the Fourier coefficients of the compensation signals. It is important to point out that the phase between the reference signals and the shaft angle is not important. Therefore the sine and the cosine could also be derived from the motor control. The only condition is that they have the same frequency as the rotation speed and the phase difference between them remains constant for a given speed.

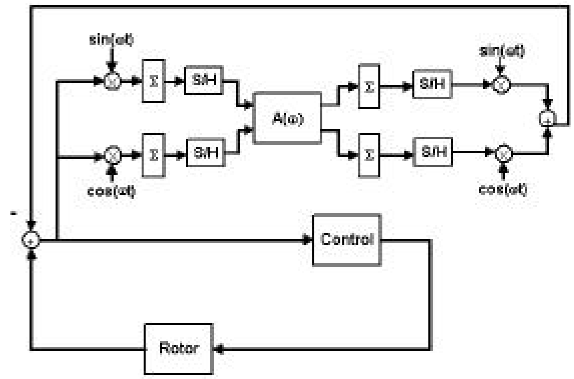

Figure 3: Structure of AVC

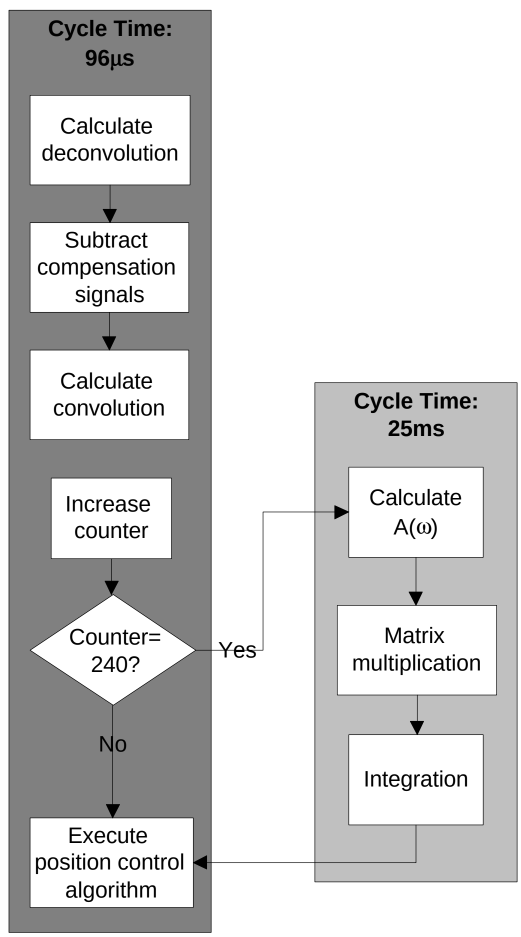

Figure 4: Flow diagram of AVC

Timing

The feedback control update rate of 10.4 kHz (see Fig. 4) is derived from an interrupt signal activated by the power electronics every PWM cycle (62.5kHz). In addition to the collection of the sensor data and the execution of the feedback control algorithm, the convolution of the performance signals is calculated. In the same cycle the Fourier coefficients of the compensation signals are transformed into time domain.
The adaptation procedure is controlled via a counter. In the actual implementation the control frequency is divided by 240 which gives an update rate for the AVC of 40Hz. In this cycle the gain matrix $\boldsymbol{A}(\omega)$ is derived from rotating speed. Based on this actual gain matrix the Fourier coefficients are updated.

Collection of the transfer matrices

To synthesize the adaptive gain matrix function, the transfer matrix $\boldsymbol{T}$ is required over the operating speed range. For this experiment these matrices were measured directly from AMB-supported rotor using a special identification algorithm with a structure similar to that of the AVC (compare Fig. 5 with Fig. 3).

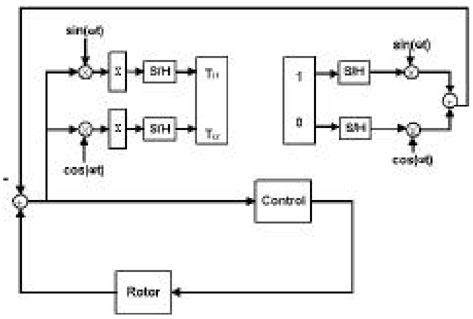

Figure 5: Modifications for estimating $\boldsymbol{T}$

This algorithm sends a set of $2n$ feedforward test Fourier vectors to the system with the rotor levitated. In order to simplify the required calculations, these test vectors are chosen to be the $2n$ columns of a $2n \times 2n$ identity matrix. These vectors are multiplied by the speed-synchronous reference sine and cosine signals to generate a series of excitation signals in exactly the same manner as AVC does. The convolution of the position sensor signals with the reference signals produces $2n$ performance Fourier vectors in response to the excitation. It is obvious that these vectors are the column vectors of the desired transfer matrix. To mitigate the effects of noise the test vectors are applied during a longer period. Empirically good results are obtained if one computes the Fourier vectors over 20 cycles. This $\boldsymbol{T}$ matrix identification may be done during operation at each speed ω_k of interest, so that any gyroscopic effects are taken into account. To be independent of the actual unbalance, the response of the system without excitation must also be measured at each speed with the resulting vector subtracted from each column vector of the obtained response matrix to yield $\boldsymbol{T}_k$.
Since the rotor examined here is not very gyroscopic, the estimation of $\boldsymbol{T}_k$ was made without the rotor turning. External reference sine and cosine were used in place of the Hall sensor signals.

RESULTS

Forty transfer matrices were measured from 10Hz to 2kHz. They were downloaded into MATLAB. The GEVP optimization was carried out on three separate speed ranges: 50-300Hz, 300-600Hz and 600-2000Hz. A linear matrix function ($\boldsymbol{A}_0$ and a_1) was found for each of these speed ranges, allowing stable adaptation between 50Hz and 2kHz.
Fig. 6 shows the measured synchronous current at the output of the position controller during run up with AVC turned off and on. At speeds below 30Hz the AVC is turned off, since the resolution of speed determination is only 10Hz. Since the two rigid body modes, which lie below 400Hz, have low damping, the AVC is very effective in this frequency range. Because of the good quality of the rotor balance the reduction in current used above 400Hz is not as significant as that below. Between 1300Hz and 1800Hz the adaptation was frozen, since synchronous current minimization cannot be performed at a bending mode natural frequency as the vibration will grow until loss of levitation occurs. Note that this is not adaptation instability since the currents would be, in fact minimized if they were not frozen. Thus, the Fourier coefficients of the compensation signals in this speed range are not updated and are the same as those used at a speed of 1300Hz. Therefore, the current rises as the rotating speed moves towards the bending critical. However, it is still significantly less with AVC than without.

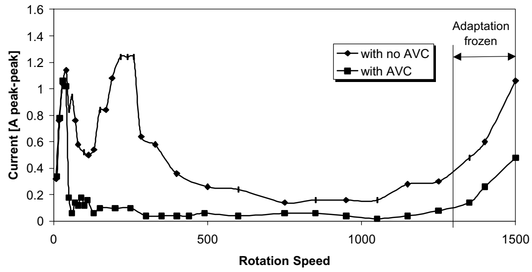

Figure 6: Synchronous currents during run up (upper bearing)

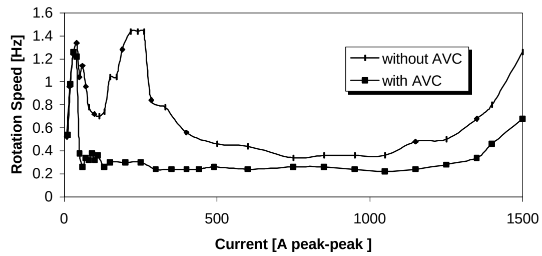

Figure 7: Bearing current during run up (upper bearing)

Fig. 7 shows the peak-to-peak bearing current which is not as low as the synchronous current. The difference between synchronous current, arises from a 0.2A current ripple, produced by the switched amplifier. The maximum peak-to-peak current employed is reduced by 90% with AVC.

Fig. 8 shows the measured displacement during run up with and without AVC. Note that the rotor turns around its axis of inertia with AVC turned on. Therefore the position is minimized since the rotor is mechanically well balanced. Thus, the 90% reduction in current used is also accompanied by a significant reduction in rotor vibration.

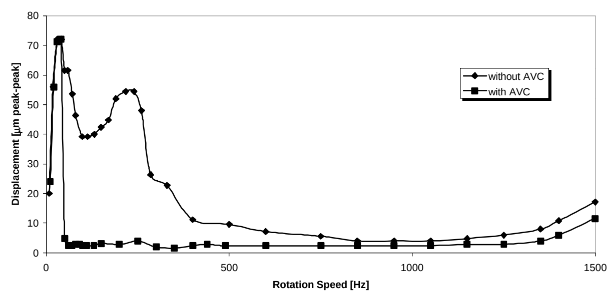

Figure 8: Unfiltered peak-to-peak displacement during run up (upper bearing)

CONCLUSIONS

In this paper a new form of the Adaptive Vibration Control algorithm is examined. To minimize the requirements on the signal electronics, this algorithm employs an adaptation gain matrix which is functionally dependent on operating speed rather than using a look-up table. This gain matrix function was synthesized using experimentally determined transfer matrices obtained at zero rotation speed. A shaft-mounted permanent magnet and two Hall sensors were also used to generate synchronous signals for convolution, significantly lowering the computational burden placed on the signal electronics. The experimental data clearly demonstrates that very high operating speeds can be reached for such AMB systems without the use of large coil currents.

ACKNOWLEDGEMENT

This project was a joint project of the University of Virginia and the Swiss Federal Institute of Technology of Zurich. It was supported by the companies Sulzer Electronics AG, Switzerland and Lust Antriebstechnik GmbH, Germany.

REFERENCES

[1] P.Gahinet, A. Nemirowski, A.J. Laub, M. Chiladi, “LMI Control Toolbox”, *The MathWorks Inc.*, 1995

[2] R. Herzog, P. Bühler, C. Gähler, R. Larsonneur, “Unbalance Compensation using Generalized Notchfilters in the Multivariable Feedback of Magnetic Bearings”, *IEEE Transactions on Control Systems Technology*, vol. 4, no. 5, 1996

[3] R. W. Hope, C. R. Knospe, “Adaptive Open Loop Control of Synchronous Rotor Vibration using Magnetic Bearings”, *University of Virginia*, Report No. UVA/643092/MAE94/475, Aug. 1994

[4] R. W. Hope, L. Tessier, C. Knospe, T. Miyamji, “Adaptive Vibration Control of Industrial Turbomachinery”, *ASME/IGTI Turbo Expo 98*, Stockholm, Sweden, June 1998

[5] C. R. Knospe, R. W. Hope, S. J. Fedigan, R. D. Williams, “A Multi- Tasking DSP Implementation of Adaptive Magnetic Bearing Control”, *IEEE Transactions on Control Systems Technology*, vol. 5, no. 2, pp. 230- 238, 1997

[6] C. R. Knospe, S. M. Tamer, S. J. Fedigan, “Synthesis of Robust Gain Matrices for Adaptive Rotor Vibration Control”, *ASME Journal of Dynamic Systems, Measurement and Control*, pp. 298-300, 1997

[7] C. R. Knospe, S. M. Tamer, R. Fittro, “Rotor Synchronous Response Control: Approaches for Addressing Speed Dependence”, *Journal of Vibration and Control*, vol. 3, pp. 435-458, Sage Publications Inc., 1997

[8] E. H. Maslen, P. E. Allaire, M. D. Noh and C. K. Sortore, “Magnetic Bearing Design for Reduced Power Consumption”, *ASME Journal of Tribology*, vol. 118, no. 4, pp. 839-846, 1996

[9] J. Schmied, F. Betschon, “ Engineering for Rotors Supported on Magnetic Bearings: The Process and the Tools”, *Proc. of the 6th ISMB*, pp. 244-255, Technomic Publishing Co. Inc., Lancaster, Basel, August 1998

[10] G. Schweitzer, H. Bleuler, A. Traxler, “ Active Magnetic Bearings”, vdf Hochschulverlag an der ETHZ, ISBN 3728121320, 1994

[11] Vacuumschmelze, “Rare-Earth Permanent Magnets”, Firmenschrift, April 1995